

1

2 **Supplementary Information for**

3 ***In situ* investigation of water on MXene Interfaces**

4 **Wahid Zaman, Ray Matsumoto, Matthew W. Thompson, Yu-Hsuan Liu, Yousuf Bootwala, Marm B. Dixit, Ethan Crumlin, Marta**
5 **C. Hatzell, Peter T. Cummings and Kelsey B. Hatzell**

6 **Kelsey B. Hatzell.**

7 **E-mail:** kelsey.hatzell@princeton.edu

8 **This PDF file includes:**

9 **Figs. S1 to S12**

10 **Tables S1 to S8**

11 **SI References**

12 **Peak fitting.** For peak fitting, CasaXPS software was used for data analysis. During spectra acquisition at 800eV, presence
 13 of Auger peaks was observed, which can be located by comparing 900eV spectra (Fig. S9). To eliminate the effect of Auger
 14 peaks, a background subtraction was carried on (for C1s). The final peaks were corrected by using Tougaard background. For
 15 best fitting, a modified asymmetric Lorentzian lineshape (LF) was chosen for O1s and C1s peaks. The rest were fitted using
 16 Gaussian Lorentzian (GL) lineshape. The XPS spectra was calibrated to TiC-T_x component of C1s spectra at 282V. It should
 17 be noted that, the Fermi edges of the MXene samples were not sharp enough to locate the 0 eV. Therefore, an alternative
 18 calibration approach was implemented by referencing to the TiC-T_x peak. Binding energies and FWHM for the peaks are
 19 listed in Table S1-S3.

20 **T_x⁻ mole number calculation.** Surface termination groups for MXene samples were determined by first calculating the global
 21 atomic percentage of all elements:

$$X_i = \frac{C_i}{\sum_{j=1}^m C_j}$$

$$C_i = \frac{I_i}{R_i}$$

22 Where X_i = Atomic fraction of element i, C_i = intensity of element i and $\sum_{j=1}^m C_j$ = Cumulative intensity of all elements, I_i =
 23 integrated area of element i, R_i = Relative sensitivity factor (RSF) of element i.

24 T_x⁻ mole numbers were calculated by taking the areal fraction of each species (-O, -F, -OH, -H₂O) from O1s and F1s spectra,
 25 multiplied by the global atomic percentage of the respective species. The amount of TiO₂ was calculated from Ti2P spectra
 26 and O-TiC from O1s was accounted from that accordingly.

27 **Relative sensitivity factor.** The relative sensitivity factors (RSFs) for beamline 9.3.2 were calculated using four correction
 28 parameters (the flux of the beamline, the analyzer transmission function, the differential cross section, and the inelastic mean
 29 free path). The flux was directly measured using a photodiode at the position of the sample and the analyzer transmission
 30 function was deduced from the intensity of Au 4f spectra of a clean gold foil at a series of excitation energies using the same
 31 data correction procedure, except for the inelastic mean free path, which was calculated with values calculated from optical
 32 properties of the elements (1). The differential cross sections were obtained by assuming random orientation of grains and using
 33 an angle between polarization vector and photoelectron direction of 20 (2). The inelastic mean free path was calculated with the
 34 predictive TPP-2M formula in an iterative manner: the material parameters entering the equation, i.e. the density, the number
 35 of valence electrons, and the molar mass, were calculated from the sum formula, which was initially guessed and improved
 36 iteratively, based on the outcome of the composition analysis. The band gap (another parameter in the TPP-2M formula) was
 37 assumed to be 0 eV. The density was calculated from the sum formula and the volume of the unit cell obtained from XRD.
 38 The effect of the volume changes on the relative sensitivity factors were negligible. Eight s- and p-orbital valence electrons of
 39 titanium are typically categorized as high-binding energy valence electrons and were not accounted for the calculation of the
 40 inelastic mean free path (3). The product of the four correction factors were normalized to the resulting values of C 1s. The
 41 RSF values for all elements are shown in Table S8.

Table S1. XPS peak fitting results of neat $\text{Ti}_3\text{C}_2\text{T}_x$ at 100 mTorr vapor pressure

Region	Temperature	BE[eV]	FWHM	Fraction	Component	Reference
Ti 2p _{3/2} (2p _{1/2})	25°C	455.07 (460.77)	1.7 (2)	0.19 (0.09)	Ti ⁺	(4)
		456.06 (461.76)	1.8 (1.74)	0.2 (0.1)	Ti ²⁺	(4)
		457.35 (463.05)	1.8 (1.68)	0.13 (0.067)	Ti ³⁺	(4)
		458.77 (464.47)	1.7 (2.28)	0.11 (0.055)	TiO ₂	(5)
		460 (465.70)	1.8 (2.97)	0.03 (0.015)	TiC-T _x	(6)
Ti 2p _{3/2} (2p _{1/2})	200°C	455 (460.7)	1.7 (2.15)	0.18 (0.09)	Ti ⁺	(4)
		456.02 (461.72)	1.8 (1.78)	0.22 (0.11)	Ti ²⁺	(4)
		457.24 (462.94)	1.7 (1.55)	0.11 (0.054)	Ti ³⁺	(4)
		458.53 (464.23)	1.72 (2.17)	0.12 (0.058)	TiO ₂	(5)
		460 (465.70)	1.8 (2.93)	0.04 (0.02)	TiC-T _x	(6)
O1s	25°C	529.80	1.58	0.3	TiO ₂	(7)
		530.70	1.62	0.3	TiC-O	(8)
		531.95	1.62	0.18	TiC-OH	(7)
		533.08	1.58	0.088	H ₂ O	(7)
		534.84	1.58	0.12	gp-H ₂ O	(7)
O1s	200°C	529.79	1.58	0.39	TiO ₂	(7)
		530.73	1.62	0.31	TiC-O	(8)
		531.94	1.62	0.17	TiC-OH	(7)
		533.08	1.58	0.044	H ₂ O	(7)
		534.78	1.58	0.087	gp-H ₂ O	(7)
C1s	25°C	282	1.3	0.494	TiC-T _x	(8)
		284.52	2.04	0.505	C-C/CH _x	(9)
C1s	200°C	281.98	1.31	0.47	TiC-T _x	(8)
		284.5	2.05	0.53	C-C/CH _x	(9)
F1s	25°C	684.9	1.63	0.9	TiC-(O,F) _x	(8)
		686.7	1.2	0.1	AlF _x	(10)
F1s	200°C	684.9	1.72	0.87	TiC-(O,F) _x	(8)
		686.82	1.54	0.13	AlF _x	(10)

Table S2. XPS peak fitting results of Li-Ti₃C₂T_x at 100 mTorr vapor pressure

Region	Temperature	BE[eV]	FWHM	Fraction	Component	Reference
Ti 2p _{3/2} (2p _{1/2})	25°C	455.05 (460.75)	1.7 (2.5)	0.10 (0.05)	Ti ⁺	(4)
		455.80 (461.50)	1.81 (1.44)	0.14 (0.07)	Ti ²⁺	(4)
		457.15 (462.85)	1.8 (1.52)	0.12 (0.059)	Ti ³⁺	(4)
		459 (464.7)	1.66 (2.38)	0.24 (0.12)	TiO ₂	(5)
		460 (465.70)	1.81 (3.2)	0.063 (0.031)	TiC-T _x	(6)
Ti 2p _{3/2} (2p _{1/2})	200°C	455.15 (460.85)	1.7 (2.42)	0.11 (0.057)	Ti ⁺	(4)
		455.75 (461.45)	1.81 (1.45)	0.12 (0.06)	Ti ²⁺	(4)
		457.07 (462.77)	1.45 (1.8)	0.13 (0.066)	Ti ³⁺	(4)
		458.97 (464.67)	1.6 (2.38)	0.25 (0.125)	TiO ₂	(5)
		460 (465.70)	1.81 (3.3)	0.05 (0.025)	TiC-T _x	(6)
O1s	25°C	530.35	1.62	0.33	TiO ₂	(7)
		531.3	1.58	0.25	TiC-O	(8)
		532.50	1.58	0.165	TiC-OH	(7)
		533.50	1.62	0.15	H ₂ O	(7)
		534.98	1.62	0.1	gp-H ₂ O	(7)
O1s	200°C	530.30	1.62	0.47	TiO ₂	(7)
		531.3	1.59	0.29	TiC-O	(8)
		532.50	1.58	0.144	TiC-OH	(7)
		533.45	1.59	0.04	H ₂ O	(7)
		534.9	1.58	0.055	gp-H ₂ O	(7)
C1s	25°C	282	1.35	0.367	TiC-T _x	(8)
		285	2.16	0.63	C-C/CH _x	(9)
C1s	200°C	282	1.38	0.373	TiC-T _x	(8)
		284.7	1.92	0.627	C-C/CH _x	(9)
F1s	25°C	685.2	1.75	0.86	TiC-(O,F) _x	(8)
		686.7	1.27	0.14	AlF _x	(10)
F1s	200°C	685.1	1.6	0.92	TiC-(O,F) _x	(8)
		687.5	1.2	0.08	AlF _x	(10)
Li1s	25°C	56.03	2	1	Li ⁺ /LiF	(11)
Li1s	200°C	56.1	2	1	Li ⁺ /LiF	(11)

Table S3. XPS peak fitting results of K-Ti₃C₂T_x at 100 mTorr vapor pressure

Region	Temperature	BE[eV]	FWHM	Fraction	Component	Reference
Ti 2p _{3/2} (2p _{1/2})	25°C	455.15 (460.85)	1.7 (2.42)	0.11 (0.057)	Ti ⁺	(4)
		455.75 (461.45)	1.81 (1.45)	0.12 (0.06)	Ti ²⁺	(4)
		457.07 (462.77)	1.45 (1.8)	0.13 (0.066)	Ti ³⁺	(4)
		458.97 (464.67)	1.6 (2.38)	0.25 (0.125)	TiO ₂	(5)
		460 (465.70)	1.81 (3.3)	0.05 (0.025)	TiC-T _x	(6)
Ti 2p _{3/2} (2p _{1/2})	200°C	455.12 (460.82)	1.7 (2.5)	0.1 (0.05)	Ti ⁺	(4)
		455.84 (461.54)	1.43 (1.78)	0.11 (0.055)	Ti ²⁺	(4)
		457.02 (462.72)	1.78 (1.68)	0.11 (0.056)	Ti ³⁺	(4)
		458.76 (464.46)	1.6 (2.3)	0.28 (0.14)	TiO ₂	(5)
		460 (465.70)	1.81 (3.02)	0.06 (0.03)	TiC-T _x	(6)
O1s	25°C	530.32	1.62	0.52	TiO ₂	(7)
		531.2	1.58	0.22	TiC-O	(8)
		532.40	1.61	0.098	TiC-OH	(7)
		533.30	1.6	0.072	H ₂ O	(7)
		534.8	1.58	0.097	gp-H ₂ O	(7)
O1s	200°C	530.26	1.62	0.57	TiO ₂	(7)
		531.2	1.58	0.27	TiC-O	(8)
		532.40	1.58	0.066	TiC-OH	(7)
		533.3	1.62	0.026	H ₂ O	(7)
		534.91	1.58	0.067	gp-H ₂ O	(7)
C1s	25°C	282	1.33	0.48	TiC-T _x	(8)
		284.95	2.3	0.52	C-C/CH _x	(9)
C1s	200°C	282	1.39	0.41	TiC-T _x	(8)
		284.84	1.94	0.59	C-C/CH _x	(9)
F1s	25°C	684.8	1.9	0.93	TiC-(O,F) _x	(8)
		686.9	1.46	0.07	AlF _x	(10)
F1s	200°C	684.81	1.92	0.8	TiC-(O,F) _x	(8)
		686.94	1.75	0.2	AlF _x	(10)
K 2p _{3/2} (2p _{1/2})	25°C	293.22 (296.26)	1.33 (1.22)	1	K ⁺	(12)
K 2p _{3/2} (2p _{1/2})	200°C	293.2 (296.24)	1.6 (1.7)	1	K ⁺	(12)

Table S4. Mole number of -O group in MXene samples at 25°C and 200°C at 1 mTorr and 100 mTorr vapor pressure

Sample	Temperature	1 mTorr	100 mTorr
Ti ₃ C ₂ T _x	25°C	0.7	0.8
	200°C	0.7	0.7
Li-Ti ₃ C ₂ T _x	25°C	0.8	0.7
	200°C	0.8	0.7
K-Ti ₃ C ₂ T _x	25°C	0.9	0.8
	200°C	0.9	0.9

Table S5. Mole number of -OH group in MXene samples at 25°C and 200°C at 1 mtorr and 100 mTorr vapor pressure

Sample	Temperature	1 mTorr	100 mTorr
Ti ₃ C ₂ T _x	25°C	0.6	0.5
	200°C	0.5	0.5
Li-Ti ₃ C ₂ T _x	25°C	0.6	0.6
	200°C	0.5	0.5
K-Ti ₃ C ₂ T _x	25°C	0.4	0.3
	200°C	0.2	0.2

Table S6. R² values for the regression analysis of areal fraction of adsorbed H₂O, -OH, -O and TiO₂ in MXenes at 100 mTorr with increasing temperature

Sample	H ₂ O	-OH	-O	TiO ₂
Ti ₃ C ₂ T _x	0.98	0.43	0.56	0.98
Li-Ti ₃ C ₂ T _x	0.94	0.87	0.99	0.97
K-Ti ₃ C ₂ T _x	0.92	0.99	0.34	0.99

Table S7. R² values for the regression analysis of areal fraction of water in MXenes at different vapor pressure

Sample	Temperature	R ²
Ti ₃ C ₂ T _x	25°C	0.98
	200°C	0.58
Li-Ti ₃ C ₂ T _x	25°C	0.99
	200°C	0.20
K-Ti ₃ C ₂ T _x	25°C	0.99
	200°C	0.75

Table S8. Relative sensitivity factors (RSF) for all elements in XPS analysis, carried out using 800eV excitation energy

Element	RSF
Ti2p	3.7
O1s	1
C1s	1
F1s	0.39
Li1s	0.03
K2p	3.4

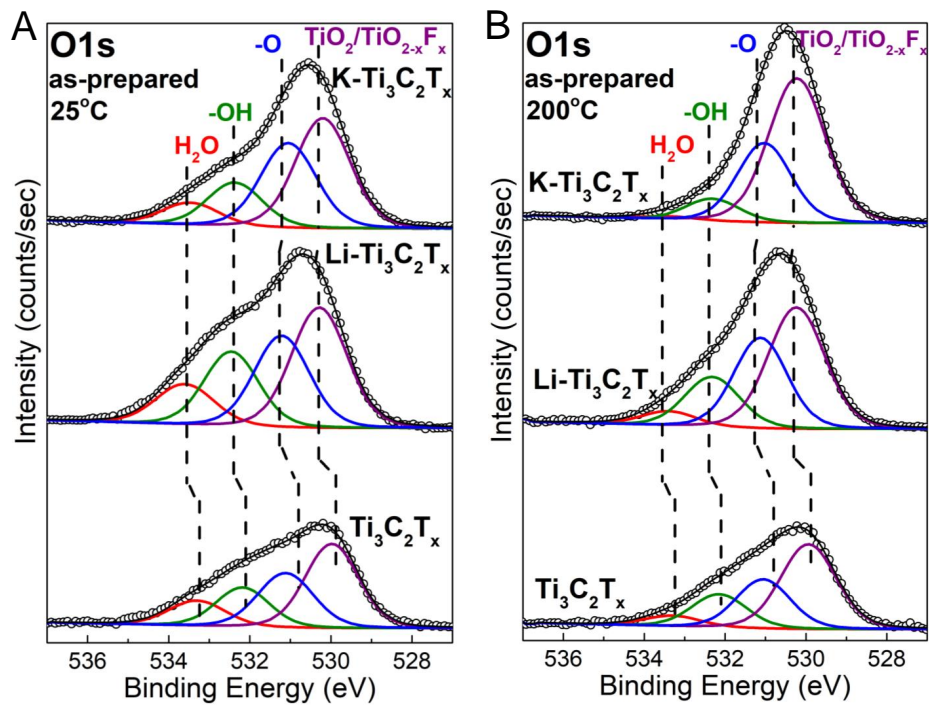


Fig. S1. O1s spectra of as-prepared samples in UHV at (a) 25°C and (b) 200°C

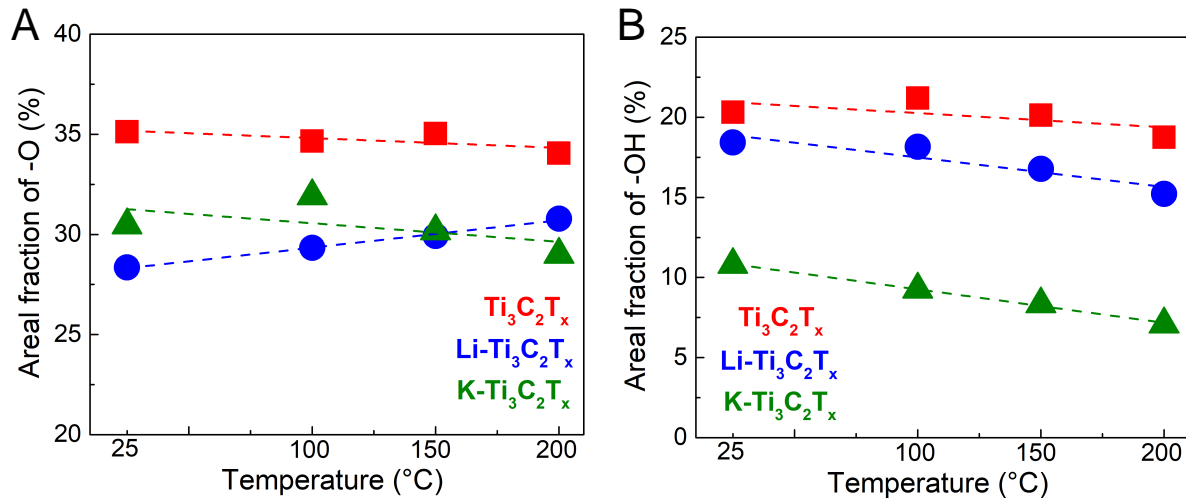


Fig. S2. O1s spectra at 100 mTorr, changes in (a)-O coverage and (b)-OH coverage with increasing temperature. The coverage in (a) and (b) was normalized with respect to the total fraction of -O, -OH, H₂O and TiO₂

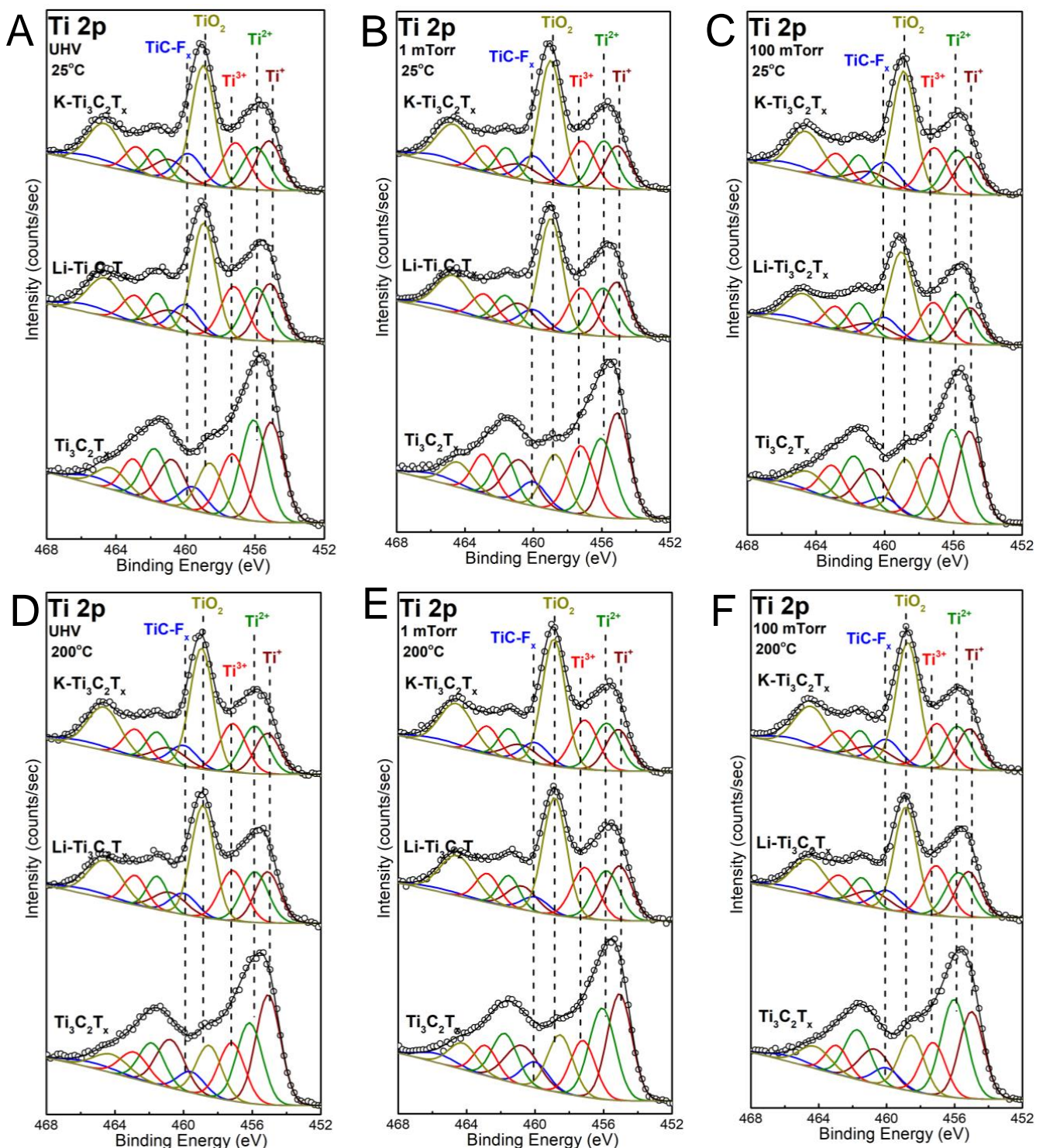


Fig. S3. Ti2p spectra at (a,d) UHV, (b,e) 1 mTorr and (c,f) 100 mTorr vapor pressure at 25°C and 200°C

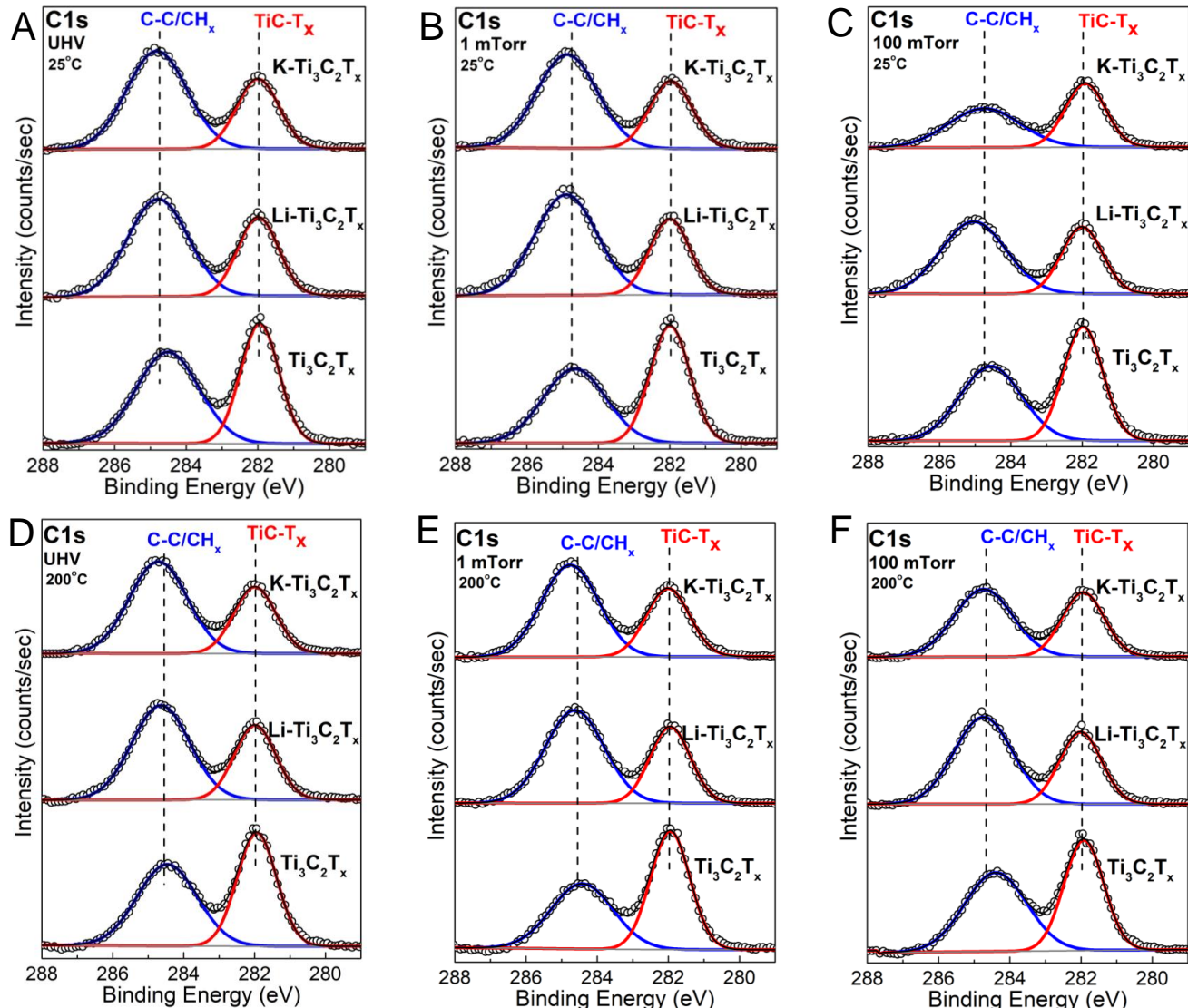


Fig. S4. C1s spectra at (a,d) UHV, (b,e) 1 mTorr and (c,f) 100 mTorr vapor pressure at 25°C and 200°C

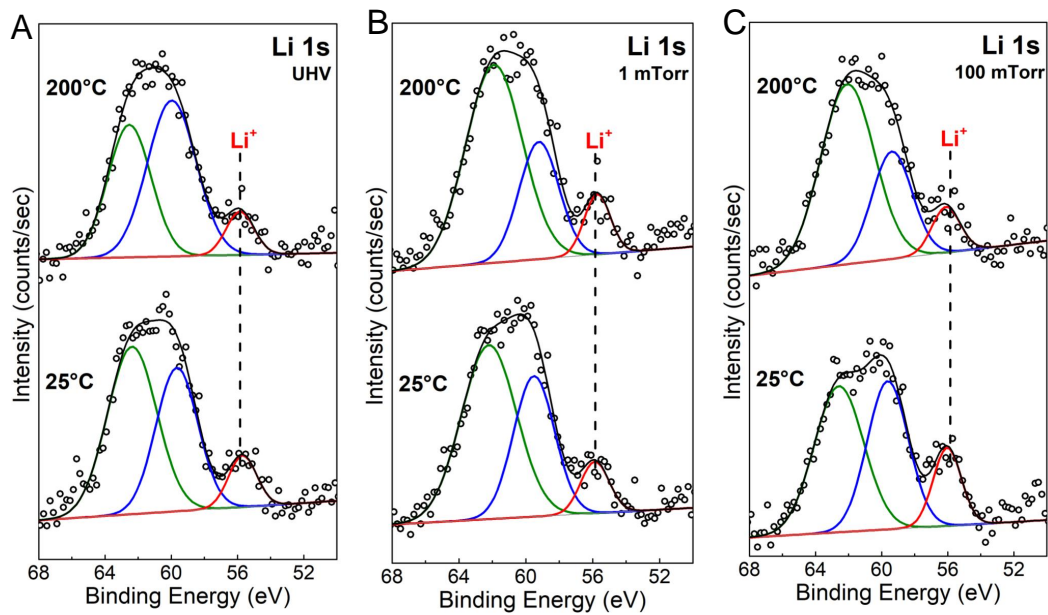


Fig. S5. Li 1s spectra at (a) UHV, (b) 1 mTorr and (c) 100 mTorr vapor pressure at 25°C and 200°C

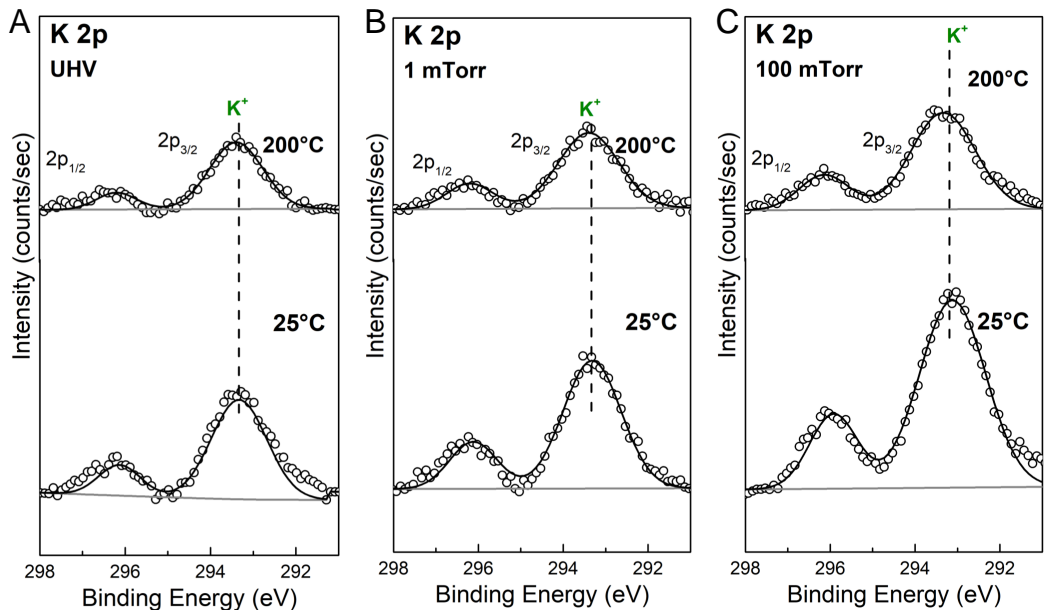


Fig. S6. K 2p spectra at (a) UHV, (b) 1 mTorr and (c) 100 mTorr vapor pressure at 25°C and 200°C

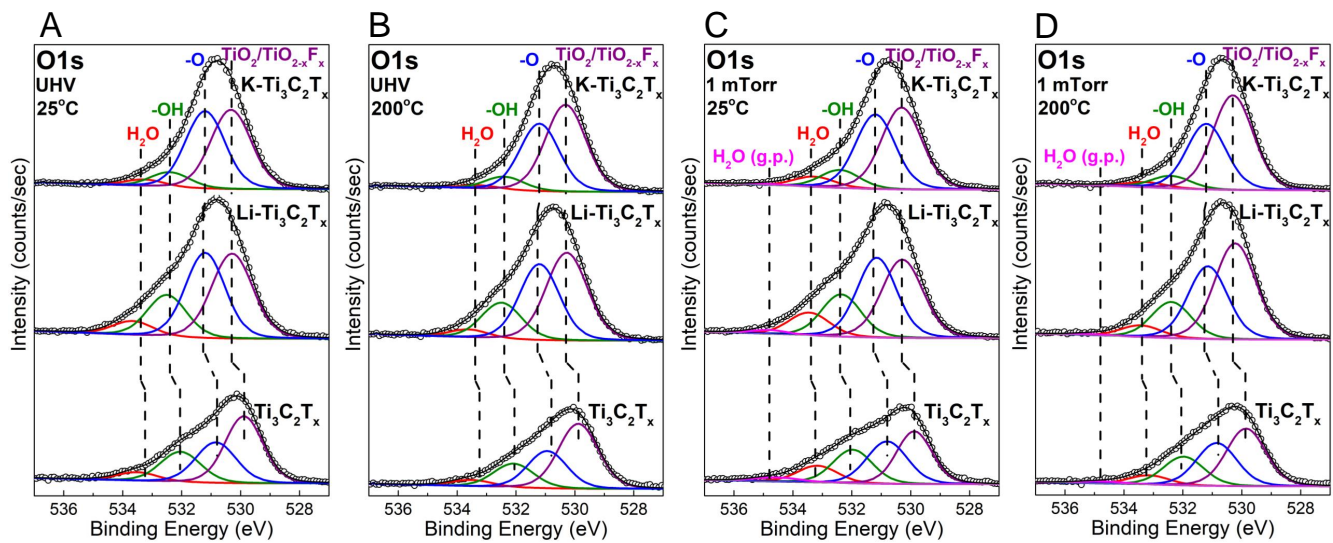


Fig. S7. O1s spectra at (a,b) UHV and (c,d) 1 mTorr vapor pressure at 25°C and 200°C

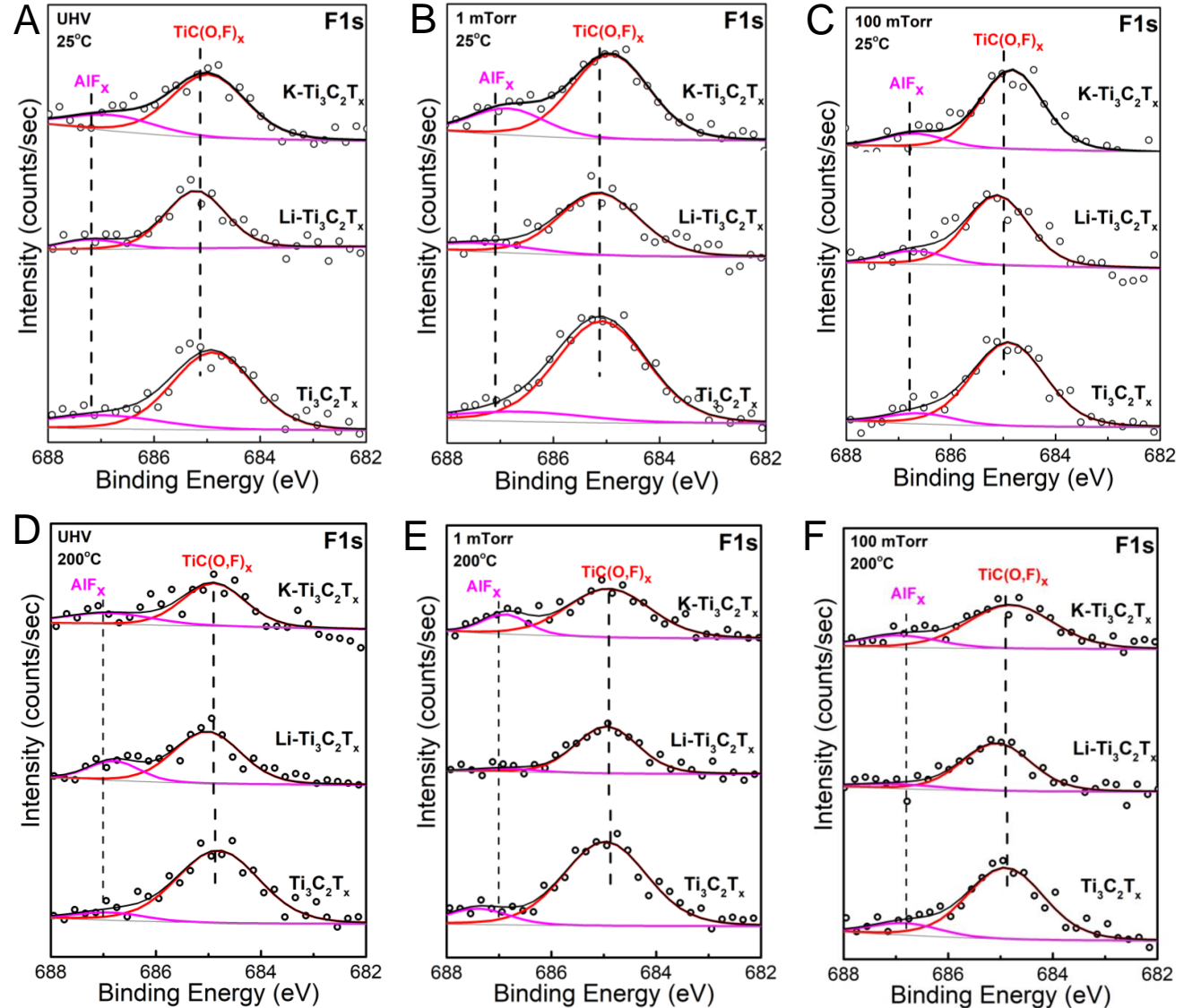


Fig. S8. F1s spectra at (a,d) UHV, (b,e) 1 mTorr and (c,f) 100 mTorr vapor pressure at 25°C and 200°C

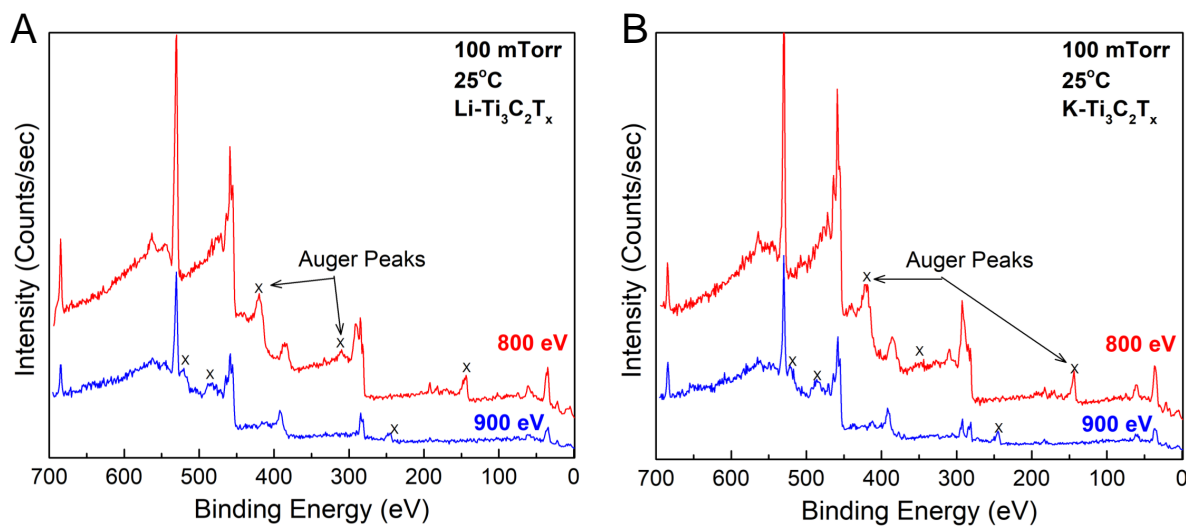


Fig. S9. Full spectra of (a) $\text{Li-Ti}_3\text{C}_2\text{T}_x$ and (b) $\text{K-Ti}_3\text{C}_2\text{T}_x$ at 800eV and 900eV showing appearance of Auger peaks

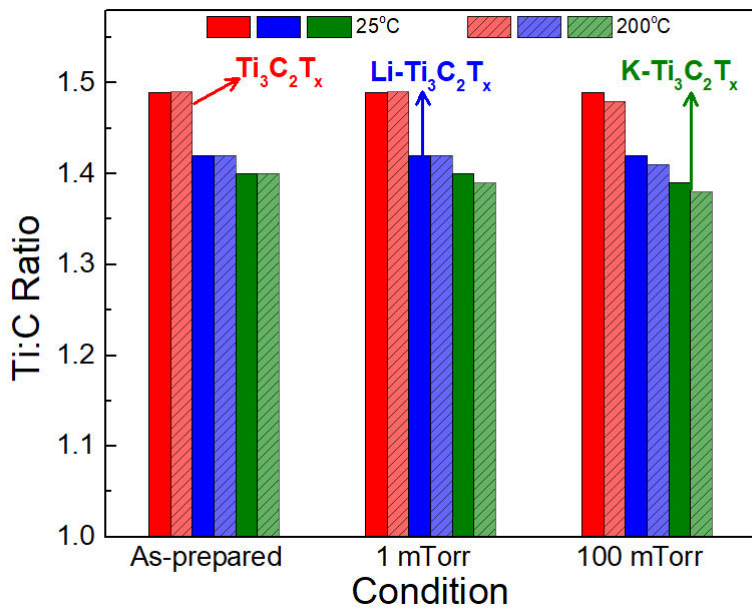


Fig. S10. Ti:C ratio of the MXenes at different conditions

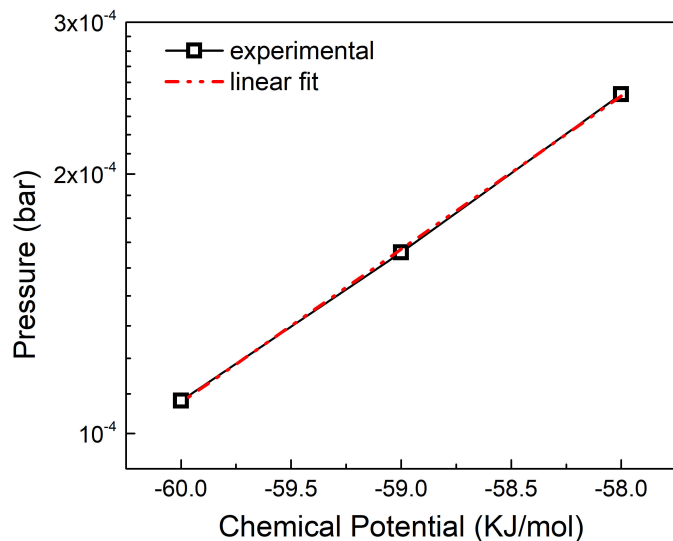


Fig. S11. Chemical Potential as a function of Pressure in a system of bulk SPC/E water

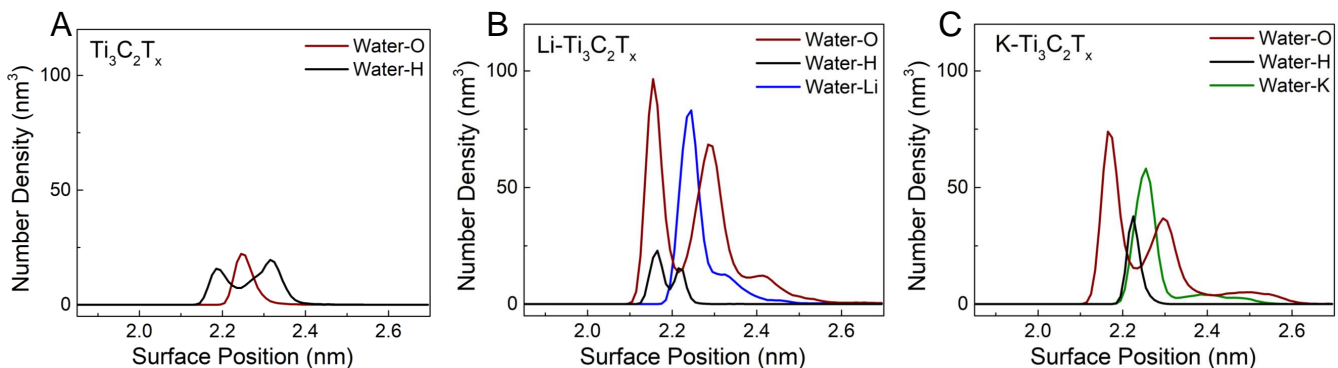


Fig. S12. Number density profiles for (a) $\text{Ti}_3\text{C}_2\text{T}_x$, (b) $\text{Li}-\text{Ti}_3\text{C}_2\text{T}_x$ and (c) $\text{K}-\text{Ti}_3\text{C}_2\text{T}_x$. Surface position at 0.0 nm corresponds to the maximum z-coordinate of the MXene sheet.

42 References

- 43 1. S Tanuma, CJ Powell, DR Penn, Calculations of electron inelastic mean free paths. IX. Data for 41 elemental solids over
44 the 50 eV to 30 keV range. *Surf. Interface Analysis* **43**, 689–713 (2011).
- 45 2. JJ Yeh, I Lindau, Atomic subshell photoionization cross sections and asymmetry parameters: $1 \leq Z \leq 103$. *At. Data Nucl.*
46 *Data Tables* **32**, 1–155 (1985).
- 47 3. NIST Standard Reference Database 71, URL: <https://www.nist.gov/srd/nist-standard-reference-database-71>. (2021).
- 48 4. V Schier, J Halbritter, K Karlsruhe, ARXPS-analysis of sputtered TiC, SiC and $\text{TiO}_2\text{SiO}_2\text{C}$ layers. *J. Anal. Chem.*,
49 227–232 (1993).
- 50 5. F Santerre, MA El Khakani, M Chaker, JP Dodelet, Properties of TiC thin films grown by pulsed laser deposition. *Appl.*
51 *Surf. Sci.* **148**, 24–33 (1999).
- 52 6. T Sultana, et al., XPS analysis of laser transmission micro-joint between poly (vinylidene fluoride) and titanium. *Appl.*
53 *Surf. Sci.* **255**, 2569–2573 (2008).
- 54 7. S Yamamoto, et al., In situ x-ray photoelectron spectroscopy studies of water on metals and oxides at ambient conditions.
55 *J. Phys. Condens. Matter* **20** (2008).
- 56 8. J Halim, et al., X-ray photoelectron spectroscopy of select multi-layered transition metal carbides (MXenes). *Appl. Surf.*
57 *Sci.* **362**, 406–417 (2016).
- 58 9. PM Jayaweera, EL Quah, H Idriss, Photoreaction of ethanol on $\text{TiO}_2(110)$ single-crystal surface. *J. Phys. Chem. C* **111**,
59 1764–1769 (2007).

- 60 10. Knst, D Grman, R Hauert, E Holländer, Fluorine-Induced corrosion of aluminium microchip bond pads: An XPS and
61 AES analysis. *Surf. Interface Analysis* **21**, 691–696 (1994).
- 62 11. M Ghidiu, et al., Ion-Exchange and Cation Solvation Reactions in Ti₃C₂ MXene. *Chem. Mater.* **28**, 3507–3514 (2016).
- 63 12. A Caballero, JP Espinós, A Fernández, L Soriano, AR González-Elipe, Adsorption and oxidation of K deposited on
64 graphite. *Surf. Sci.* **364**, 253–265 (1996).